

LncRNA XIST promotes proliferation and epithelial-mesenchymal transition of retinoblastoma cells through sponge action of miR-142-5p

C. XU, L.-H. TIAN

Department of Ophthalmology, Shanxian Central Hospital, Heze, Shandong, China

Abstract. – OBJECTIVE: The aim of the study was to investigate the effect of lncRNA XIST on the proliferation and epithelial-mesenchymal transition (EMT) of retinoblastoma (RB) and its relevant mechanism.

PATIENTS AND METHODS: 60 RB patients who were treated in our hospital were collected. The expression of XIST in tissues and cells was detected by qRT-PCR, and the effect of XIST on the prognosis of RB cells was observed. Stable and transient over-expression and suppression vectors were established and transfected into RB cells WERI-RB1 and Y79. CCK-8, transwell, and flow cytometry were used to evaluate the proliferation, invasion, and apoptosis of transfected cells. Western Blot was used to detect apoptosis-related proteins and EMT-related proteins. Dual-Luciferase report was used to determine the relationship between XIST and miR-142-5p. RNA pull-down and RIP experiments were used to determine the relationship between XIST and miR-142-5p.

RESULTS: XIST was highly expressed in RB patients, which had a high diagnostic value. Patients with XIST high expression had a poor prognosis. After overexpression of XIST, the proliferation, invasion and EMT of cells increased, and apoptosis rate decreased, while inhibition of Ptv1 had the opposite effect. Dual-Luciferase report confirmed that XIST could target miR-142-5p. Functional analysis showed that the overexpression of miR-142-5p inhibited the proliferation, invasion and EMT of RB cells and promoted cell apoptosis. Rescue experiments showed that miR-142-5p could eliminate the inhibition of miR-142-5p on the proliferation, invasion, and EMT of RB cells by upregulating XIST expression.

CONCLUSIONS: Ptv1 can promote the proliferation, invasion, and EMT of RB cells by regulating miR-142-5p.

Key Words:

LncRNA XIST, MiR-142-5p, RB, Proliferation, Invasion, Epithelial-mesenchymal transition.

Introduction

Retinoblastoma (RB) is the most common intraocular malignant tumor in children. Globally, there are approximately 20,000 new confirmed cases per year^{1,2}. In recent years, with the progress of medical technology, the diagnosis and treatment of cancer has also made great progress. Since the site of the onset of RB is close to the brain, the tumors of many RB patients are easy to metastasize to the central nervous system, leading to the poor prognosis in many patients, which poses a serious threat to the life and health of infants and children^{3,4}. Therefore, it is of great clinical significance to explore the pathogenesis of RB for the development of new diagnosis and treatment strategies.

LncRNA is an RNA with a length of about 200 nucleotides, which can be used as a transcription regulator to regulate target genes from the transcription level, thus affecting cell functions⁵. At present, the research on LncRNA is still at an initial stage compared with miRNA. LncRNA plays an important role in many diseases, including tumors^{6,7}. LncRNA XIST is one of the earliest LncRNAs found in mammals, which plays a vital role in the differentiation and proliferation of human cells⁸. There are also many studies on XIST in tumors. Cui et al⁹ have reported that XIST can promote the development of laryngeal squamous cell carcinoma by stimulating miR-144 to regulate the expression of IRS1. Cheng et al¹⁰ have found that XIST can affect the growth and glucose metabolism of RB cells by sponge acting on miR-126. Hu et al¹¹ have observed that XIST can inhibit the development and progression of RB by regulating miR-124/STAT3 axis. However, the other targets are not explained much. We found a combining site between miR-142-5p and XIST

through bioinformatics analysis. Venkatesan et al¹² have also pointed out that miR-142-5p was reduced in RB. Therefore, we suspected that XIST might also have a sponge effect on miR-142-5p to impact the development and progression of RB.

In this research, we explored the expression, function and related mechanism of XIST in RB, hoping to provide a new target direction for the diagnosis and therapy of RB.

Patients and Methods

Clinical Data

From January 2015 to October 2016, 87 children who underwent RB enucleation in our hospital were collected. The average age of all children was (59.42±4.15). 87 RB tissues were obtained as the research group with the agreement of the patients during the operation. In addition, 53 normal retinal tissues were obtained as the control group with the agreement of the patients during the eyeball enucleation for patients with accidental eyeball rupture. They were stored in a liquid nitrogen jar.

Inclusion criteria: patients were diagnosed as RB by imaging and pathological diagnosis; patients met the diagnostic evaluation requirements of retinoblastoma proposed by the European Retinoblastoma Imaging Collaboration (ERIC)¹³.

Exclusion criteria: patients who had received radiotherapy and chemotherapy were excluded; patients with other malignant tumors were excluded; patients with severe renal dysfunction were excluded; patients with serious infectious diseases were excluded; patients who refused to provide experimental specimens were excluded. This study was approved by the Ethics Committee of Shanxian Central Hospital. All patients agreed to join the test and signed an informed consent form. All patients and their families agreed to join the test and signed an informed consent form. This study was approved by the Ethics Committee of Shanxian Central Hospital.

Cell Culture and Transfection

Human retinoblastoma cell lines WERI-RB1, SO-RB50, Y79, HXO-RB44, and human retinal pigment epithelial cell line ARPE-19 (ATCC, Manassas, VA, USA) were placed in Roswell Park Memorial Institute-1640 (RPMI-1640) medium (Invitrogen, Carlsbad, CA, USA) incorporating 10% phosphate-buffered saline (PBS; Gibco, Rockville, MD, USA), 2 ml penicillin and streptomycin (Invitrogen, Carlsbad, CA, USA). Finally, they were placed in an incubator at 37°C and 5% CO₂ for culture. When the adherent growth and fusion of cells were observed to reach 85%, 25% pancreatin was added for digestion. After digestion, the cells were placed in the medium for continuous culture to complete passage. WERI-RB1 and Y79 cells were transfected with Lipofectamine 2000 (Invitrogen, Carlsbad, CA, USA). The inhibitory and overexpression plasmids were established with pcDNA3.1 vector respectively. The blank vector was used as negative control. The cells were inoculated in 96-well plate and transfected for 48 hours. The transfected cells were used for further determination.

Real-Time Quantitative PCR

Firstly, the total RNA in tissues and cells was obtained with TRIzol reagent. Then, 5 µg of total RNA was fetched respectively for reverse transcription of cDNA according to the instructions of the kit. The each 1 µL of synthesized cDNA was taken for PCR after transcription. The PCR reaction parameters were as below: pre-denaturation at 95°C for 10 s, denaturation at 94°C for 10 s, anneal and extension at 60°C for 30 s, with 40 cycles. 3 multiple pores were set up for each sample, and the test was carried out for 3 times. MiR-135a used U6 as internal reference and XIST used GAPDH as internal reference. 2^{-ΔΔct} was applied to analyze the data (Table I).

Cell Proliferation Test

Cell proliferation was tested according to CCK-8 kit instructions. After transfection for 48

Table I. Primer sequences.

	Forward primer 5'-3'	Reverse primer
XIST	CTCTCCATTGGGTTTAC	GCGGCAGGTCTTAAGAGATGA
miR-142-5p	GGCCCATAAAGTAGAAAGC	TTTGGCACTAGCACATT
U6	CTCGCTTCGGCAGCAC	AACGCTTACGAATTTGCGT
GAPDH	AAGGTGAAGGTCGGAGTCAA'	AATGAAGGGGGCATTGATGG

hours, the cells were collected, diluted to 3×10^4 cell/ml, and inoculated into 96-well plates. 100 μ l of cells was inoculated to each well, cultured at 37°C and 5% CO₂. 10 μ l of CCK-8 solution was put in each well at 0 h, 24 h, 48 h, and 72 h after the cells grew adhesion to the bottom. The reagent was added, and then, the cells were cultivated for 2 h in an incubator at 37°C and 5% CO₂. Then, OD value was measured at 450 nm by enzyme-labeling instrument to detect cell proliferation and draw growth curves. The experiment was repeated for 3 times.

Cell Invasion Experiment

Transwell kit was used to test the invasion ability of cells. 200 μ L of Dulbecco's Modified Eagle's Medium (DMEM) culture solution containing 3×10^4 cells was put in the upper chamber. 500 mL of DMEM containing 20% FBS was put in the lower chamber and cultivated at 37°C for 48 h. The stroma and cells that did not pass through the membrane surface in the upper chamber were wiped, washed with fetal bovine serum (FBS) for 3 times, fastened with paraformaldehyde for 10 min, washed with double distilled water for 3 times, and stained with 0.1% crystal violet for 10 min after drying. The cell invasion was observed by microscope.

Apoptosis Experiments

Transfected cells were digested by 0.25% trypsinase, and then, washed twice by PBS. 100 μ L of binding buffer was added to prepare into 1×10^6 cells/mL suspension. AnnexinV-FITC and PI were successively put and incubated at ambient temperature and in the dark for 5 min. FACSVerse flow cytometry was used for detection. The experiment was repeated for 3 times to take the average.

Western Blot Detection

Firstly, RIPA lysate was used to extract the total protein in cells. Then, bicinchoninic acid assay (BCA) was used to detect the protein concentration. The protein concentration was adjusted to 4 μ g/ μ L, isolated by 12% sodium dodecyl sulphate-polyacrylamide gel electrophoresis (SDS-PAGE) electrophoresis, and transferred to polyvinylidene difluoride (PVDF) membrane after ionization. Then, the PVDF membrane was closed with 5% skimmed milk powder for 2 h. Next, N-cadherin (1:500), E-cadherin (1: 500), vimentin (1:500), Bax (1:500), Caspase-3 (1:500), Bcl-2 (1:500), and β -actin (1: 1000) primary anti-

body (Cell Signaling Technology, Danvers, MA, USA) were added and sealed overnight at 4°C. The primary antibody was removed by washing film. Horseradish peroxidase (HRP)-labeled goat anti-rabbit secondary antibody (1:1000; BOSTER Biological Technology Co. Ltd., Wuhan, China) was added, cultivated at 37°C for 1 h, and rinsed with TBST for 3 times for 5 min each time. It was developed in the darkroom and excess liquid on the membrane was sucked dry with filter paper. Enhanced chemiluminescence (ECL) was used to glow and develop.

Dual-Luciferase Assay

The bioinformatics database StarBase v2.0 was applied to search for candidate miRNA that can bind to XIST. Oligonucleotide containing XIST target sequence was amplified and cloned into pmirGLO plasmid (WT). pmirGLO-XIST-3'UTR wild type (Wt) and pmirGLO-XIST-3'UTR mutant (Mut) were established respectively and transferred to the downstream of Luciferase reporter gene to sequence and identify the constructed plasmid. The Luciferase reporter plasmid and miR-142-5p-mimc or miR-NC were co-transfected into Y79 cells by Lipofectamine 2000. After 24 h of culture, the cells were collected. The Luciferase activity of cells was detected by Luciferase detection kit, and the results were counted and analyzed.

RNA Pull-Down Test

Magnetic ribonucleic acid protein pull-down kit (Pierce, Rockford, IL, USA) was used. 1 μ g of biotin labeled PTV1 was put into Eppendorf (EP, Hamburg, Germany) test tube. Then, 500 μ L of structural buffer was added, and bathing was carried out at 95°C for 2 min, followed by ice bath for 3 min. 50 μ L fully resuspended beads were incubated overnight at 4°C in EP tube. Subsequently, the beads were centrifuged at 1500 xg for 3 min, and the supernatant was discarded. Then, co-immunoprecipitation was conducted by 500 μ L RNA binding protein. It was washed by RIP cleaning solution for 3 times. After washing, 10 μ L of cell lysate was put and placed at ambient temperature for 1 hour. Then, the cultured bead-RNA-protein mixture was centrifuged at low velocity. After centrifugation, the supernatant was washed for three times with 500 μ L of RIP washing buffer. The supernatant of 10 μ L cell lysate was applied as the input protein, and the protein expression was detected. The test was repeated for 3 times.

RIP Assay

RIP assay was performed in RB cells by Magna RIP RNA binding protein immunoprecipitation kit (Millipore, Billerica, MA, USA). The cells were washed with PBS and RIP lysis buffer was put. Then, the suspension was centrifuged to extract the supernatant. One part of the cell extract was applied for Input, and the other part was cultivated with antibody for coprecipitation. Each coprecipitated reaction system was washed with 50 μ L of beads and suspended in 100 μ L of RIP washing buffer. The magnetic bead-antibody complex was washed and suspended in 900 μ L of RIP washing buffer, and then, cultivated overnight at 4°C with 100 μ L of cell extract. Then, the sample was laid up on a magnetic substrate to collect magnetic globin complexes. Finally, protease K was used for sample digestion and RNA extraction for Western Blot assay. The antibody for RIP assay was AGO2 (1: 2000, Abcam, Cambridge, MA, USA), and immunoglobulin G (IgG; 1: 1000, Abcam, Cambridge, MA, USA) was applied as negative control. The test was reduplicated for three times.

Statistical Analysis

In this research, SPSS 19.0 (IBM Corp., Armonk, NY, USA) was applied to carry out

analysis on the data. GraphPad 7 (La Jolla, CA, USA) was used to draw the required pictures. Independent *t*-test was used for inter-group comparison. One-way ANOVA was applied for multi-group comparison. LSD-t test was applied for pairwise comparison afterwards. Repetitive measurement and analysis of variance was used for multi-time point expression. Bonferroni was used for back testing. There was statistical difference with $p < 0.05$.

Results

XIST Was Enhanced In RB Tissues and Cells

Through detection, it was concluded that XIST was highly expressed in RB tissues and cells, and miR-142-5p was lowly expressed in RB tissues and cells. The analysis of receiver operating characteristics curve showed that the area under XIST curve was 0.929. According to the median value of XIST, it was separated into high and low expression groups (46/41), and it revealed that the 3-year survival rate of patients with XIST high expression was lower than that of patients with low expression ($p < 0.05$). More details are shown in Figure 1.

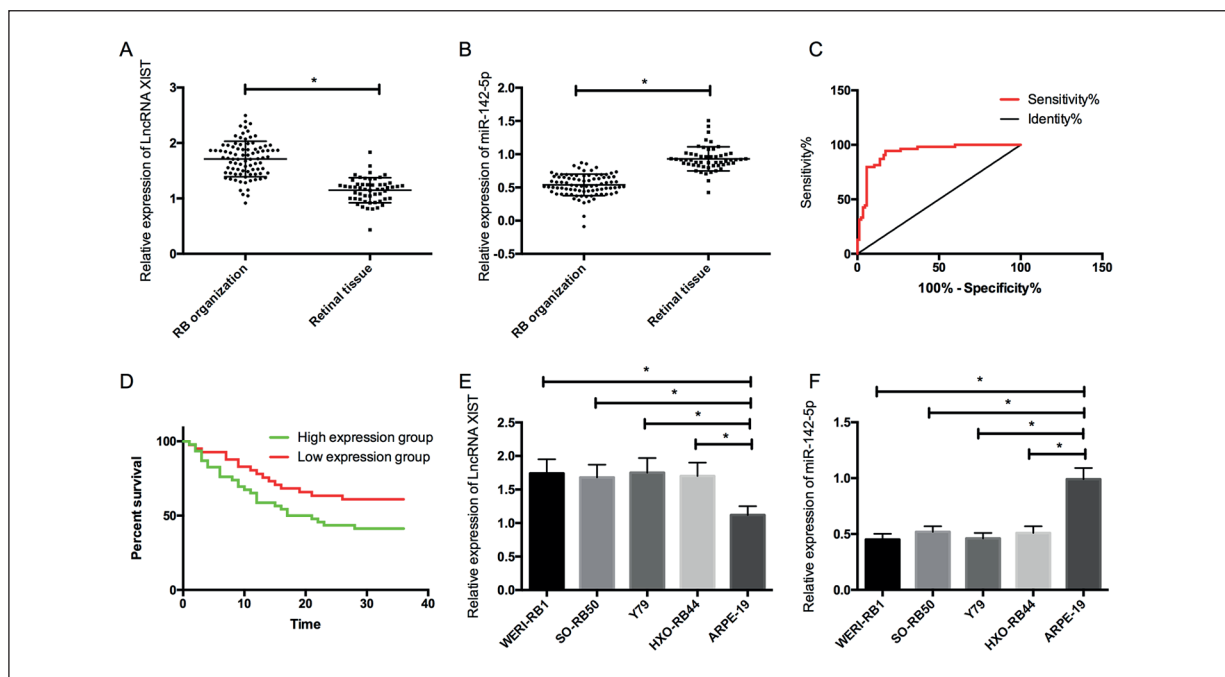


Figure 1. Expression and clinical significance of XIST in RB. **A**, Expression of XIST in RB tissue. **B**, Expression of miR-142-5p in RB tissue. **C**, ROC curve analysis of XIST to RB. **D**, Influence of XIST on prognosis of RB patients. **E**, Expression of XIST in RB cells. **F**, Expression of miR-142-3p in RB cells. * means $p < 0.05$.

Impact of XIST on Growth, Invasion, Apoptosis and EMT of RB Cells

After transfection of WERI-RB1 and Y79 cells with Si-XIST and Sh-XIST, it was found that the expression of XIST in cells transfected with Si-XIST was markedly lower than that in cells transfected with miR-NC, while the expression of XIST in cells transfected with Sh-XIST was markedly higher than that in cells transfected with miR-NC. Detection of the biological functions of cells in the two groups revealed that the growth and invasion ability of transfected Si-XIST cells were significantly reduced compared with miR-NC, but the apoptosis rate was significantly increased, the expressions of Bax, Caspase-3, E-Cadherin proteins were significantly increased, while the expressions of Bcl-2, N-cadherin, vimentin proteins were significantly decreased ($p < 0.05$). However, compared with miR-NC, the proliferation and invasion ability of transfected Sh-XIST cells increased significantly, the apoptosis rate reduced significantly, the expression of Bax, Caspase-3 and E-Cadherin proteins decreased markedly, and the Bcl-2, N-cadherin and vimentin proteins expression enhanced ($p < 0.05$). More details are shown in Figure 2.

Impacts of MiR-142-5p on Proliferation, Invasion, Apoptosis and EMT of RB Cells

After transfection of WERI-RB1 and Y79 cells with miR-142-5p-mimics, miR-142-5p-inhibitor and miR-NC, it was found that the miR-142-5p expression in cells transfected with miR-142-5p-mimics was significantly higher than that in cells transfected with miR-NC, while the miR-142-5p expression in cells transfected with miR-142-5p-inhibitor was significantly lower than that in the cells transfected with miR-NC. Detection of the biological functions of cells in the two groups, it was found that the proliferation and invasion ability of transfected miR-142-5p-mimics cells were markedly reduced compared with miR-NC, but the apoptosis rate was significantly increased, the expressions of Bax, Caspase-3, E-Cadherin proteins were significantly increased, and the expressions of Bcl-2, N-cadherin, vimentin proteins were significantly decreased ($p < 0.05$). However, compared with miR-NC, the proliferation and invasion ability of transfected miR-142-5p-inhibitor cells increased significantly, the apoptosis rate reduced significantly, the expression of Bax, Caspase-3, and E-Cadher-

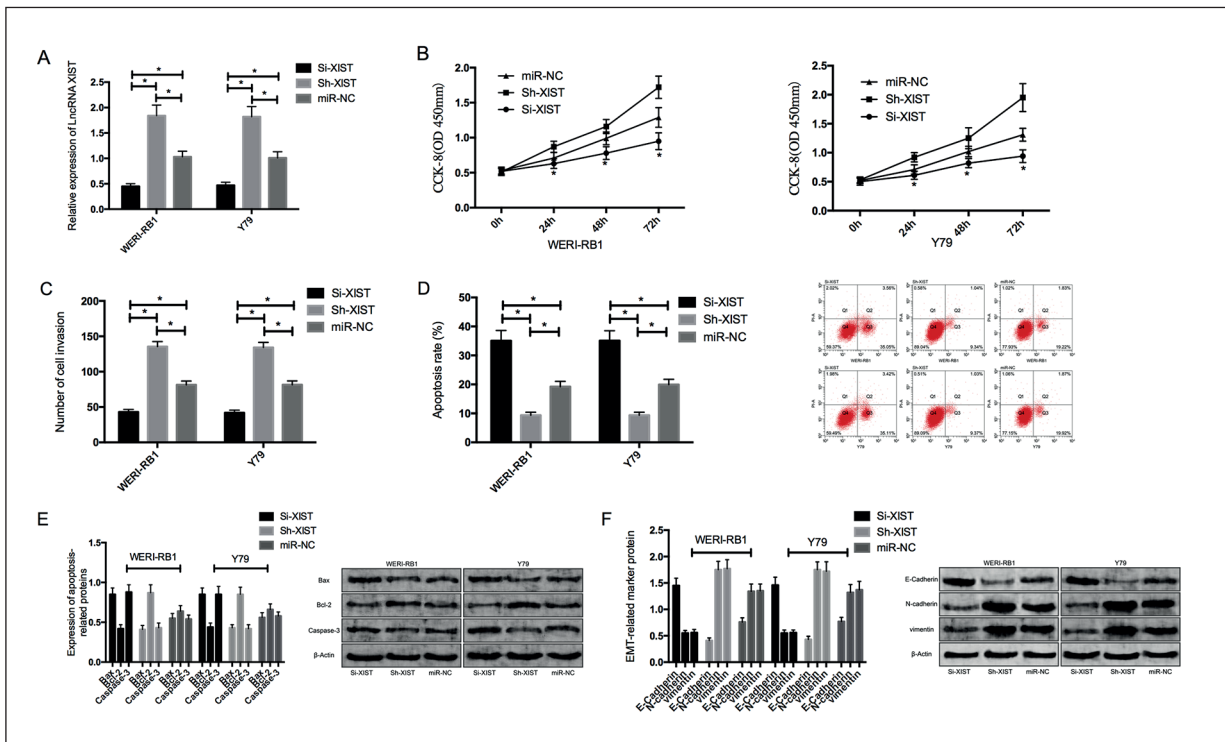


Figure 2. Effect of XIST on biological function of RB cells. **A**, Expression of XIST in RB cells after transfection. **B**, Effect of XIST on proliferation of RB cells. **C**, Effect of XIST on invasion ability of RB cells. **D**, Effect of XIST on apoptosis rate of RB cells. **E**, Effect of XIST on apoptosis related proteins in RB cells. **F**, Effect of XIST on EMT-related proteins in RB cells. * means $p < 0.05$.

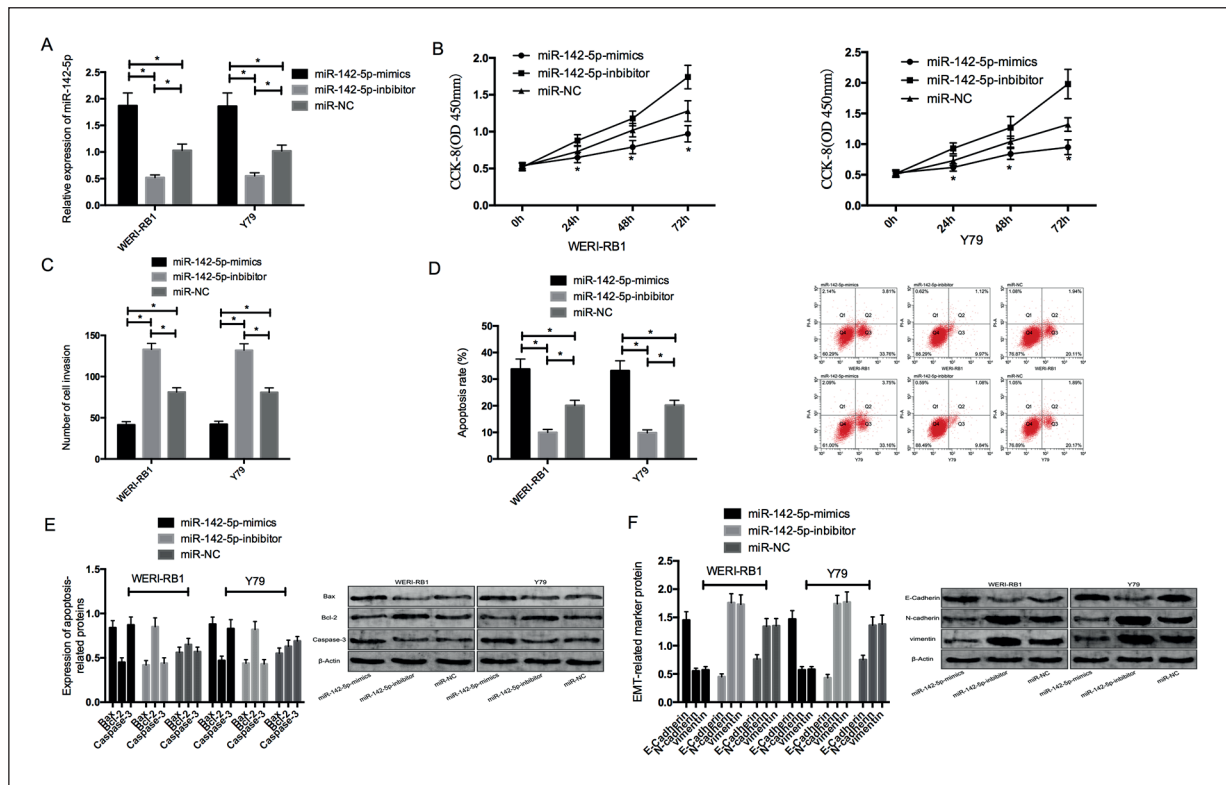


Figure 3. Expression of miR-142-3p on biological function of RB cells. **A**, Expression of miR-142-5p in RB cells after transfection. **B**, Effect of miR-142-5p on proliferation of RB cells. **C**, Effect of miR-142-5p on the invasive ability of RB cells. **D**, Effect of miR-142-5p on apoptosis rate of RB cells. **E**, Effect of miR-142-5p on apoptosis related proteins in RB cells. **F**, Effect of miR-142-5p on EMT-related proteins in RB cells. * means $p < 0.05$.

in proteins markedly decreased, and the Bcl-2, N-cadherin, and vimentin proteins expression significantly enhanced ($p < 0.05$). More details are shown in Figure 3.

LncRNA XIST Acted As a Molecular Sponge for MiR-142-5p In RB Cells

The targeted combining site between LncRNA XIST and miR-142-5p was concluded through the analysis of online software starBase 3.0. Further, the Dual-Luciferase report detection found that the miR-142-5p Luciferase activity in XIST-WT was significantly reduced and miR-NC group. The RNA pull-down test found that the enrichment of XIST in AGO2 increased compared with IgG, indicating that XIST can bind to AGO2. RIP experiments showed that miR-142-5p-WT and XIST are enriched more than miR-NC and miR-142-5p-MUT. More details are shown in Figure 4.

Rescue Experiments

By co-transfection of WERI-RB1 and Y79 cells with Si-XIST+miR-142-5p-inhibitor, the

growth, invasion, apoptosis, and EMT of cells were detected. This results showed that the proliferation, invasion, apoptosis, and EMT of transfected Si-XIST+miR-142-5p-inhibitor cells were not different from those of transfected miR-NC cells. The transfection of Si-XIST could reverse the promotion of miR-142-5p-inhibitor on cell growth, invasion, and EMT and inhibition of it on cell apoptosis. More details are shown in Figure 5.

Discussion

In recent years, LncRNA has been gradually found to play a very important role in various diseases, including tumors, and XIST has also been proved to be upregulated in many tumors^{14,15}. Chen et al¹⁶ have found that XIST can promote the development of esophageal cancer by sponge acting on miR-494. In our study, we also found that compared with normal retinal tissues, the XIST expression in RB tissues was markedly up-

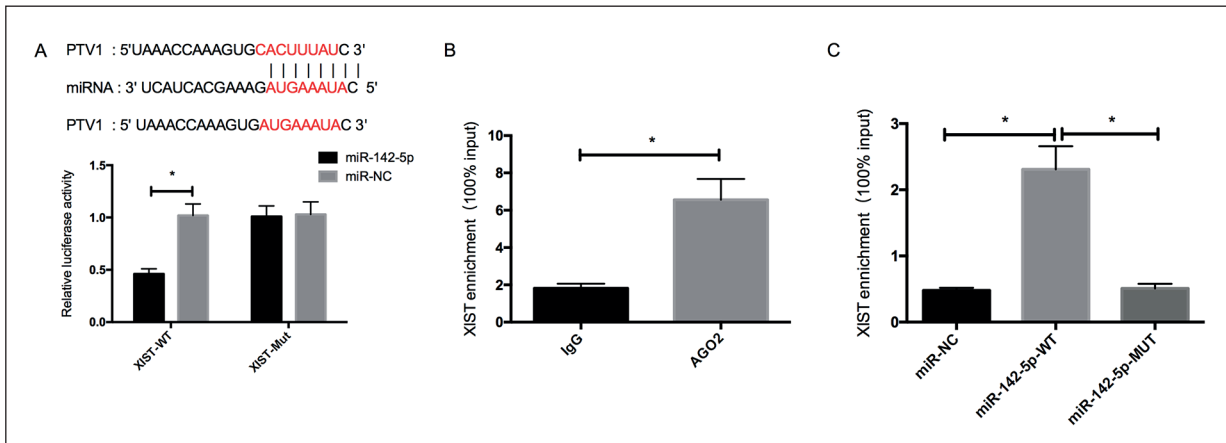


Figure 4. Relationship between XIST and miR-142-5p. **A**, Dual-Luciferase report confirmed that XIST had binding relationship with miR-142-5p. **B**, The enrichment capacity of XIST and AGO2 was evaluated and tested by RIP. **C**, The enrichment capacity of XIST and miR-142-5p was determined by RNA pull-down. * means $p < 0.05$.

regulated, which was consistent with the expression of XIST in many other tumors. The clinical significance of XIST in RB was analyzed, and it was found that XIST not only had certain diagnostic value for RB, but also the increase of its expression was related to the poor prognosis of

RB patients. All these suggested that XIST might play the role of oncogene in RB.

However, expression detection alone is not sufficient to prove our conclusion. Although it has been found that XIST played a role of oncogenic gene in most tumors, Wang et al¹⁷ have found that

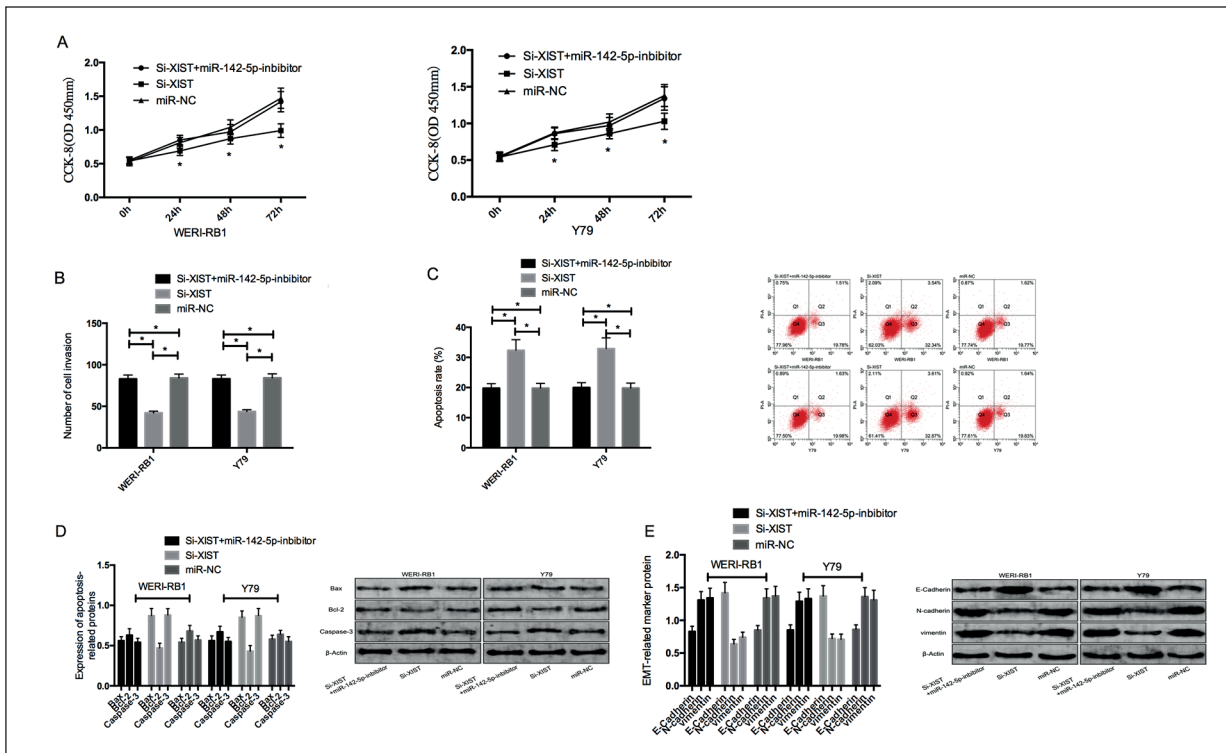


Figure 5. Rescue experiments. **A**, Effect of co-transfection of Si-XIST+miR-142-5p-inhibitor on proliferation of RB cells. **B**, Effect of co-transfection of Si-XIST+miR-142-5p-inhibitor on the invasion of RB cells. **C**, Effect of co-transfection of Si-XIST+miR-142-5p-inhibitor on apoptosis rate of RB cells. **D**, Effect of co-transfection of Si-XIST+miR-142-5p-inhibitor on apoptosis related proteins of RB cells. **E**, Effect of co-transfection of Si-XIST+miR-142-5p-inhibitor on EMT-related proteins in RB cells.

XIST is reduced in ovarian cancer and acts as a tumor suppressor. This contradiction has also suggested that XIST may play different roles in different tumors. Therefore, in order to further determine the action of XIST in RB, we intervened the XIST expression in RB cells. This results revealed that when the XIST expression was knocked down, the growth and invasion of RB cells were significantly inhibited, and the apoptosis rate was significantly enhanced. RB can easily spread to the brain through optic nerve after occurrence so as to cause distant metastasis. The occurrence of EMT is a key step for tumor metastasis¹⁸. EMT is a marker of cellular invasiveness and it has been widely recognized as a key process involved in distant metastasis¹⁹. The decrease or loss of E-cadherin is a well-known marker of EMT, and the downregulation of E-cadherin is related to the poor clinical prognosis of many cancers²⁰. Consistent with the results of cell migration and invasion, the knockdown of XIST increased the expression of the epithelial marker E-cadherin, but it decreased the expression of the mesenchymal marker N-cadherin, indicating that the EMT of RB cells was significantly inhibited. However, when the XIST expression was further enhanced, the proliferation, invasion and EMT of RB cells were significantly raised, and the apoptosis rate was significantly declined. Bax, Bcl-2, and Caspase-3 were apoptosis-related proteins, and their expression changes also usually reflect the apoptosis state of cells²¹. The expression changes of Bax, Bcl-2 and Caspase-3 proteins were also consistent with the changes of apoptosis rate. All these results suggested that XIST played an oncogenic role in RB.

It is well known that lncRNA can exert its function on cells by acting as ceRNA of miRNA²². To further seek the possible mechanism of XIST in RB, we predicted that XIST had a binding site with miR-142-5p through the online database StarBase, and confirmed the targeting relationship between XIST and miR-142-5p through double fluorescein reporter RIP and pull-down experiments. In the past, miR-142-5p has been revealed to play a role as a tumor suppressor gene in numerous tumors. Of note, Yao et al²³ have revealed that miR-142-5p can control the occurrence and development of pancreatic cancer by targeted regulation of RAPA. Wang et al²⁴ have revealed that miR-142-5p can control the occurrence of tumors by targeting PIK3CA in non-small cell lung cancer. In our research, we concluded that miR-142-5p was low expressed in RB. In the past, some studies²⁵ have

also revealed that miR-142-5p is lowly expressed in RB, which is consistent with our results. However, there is no further research on the specific impact of miR-142-5p on RB cells. Therefore, the miR-142-5p expression in RB cells was also regulated in our experiment, and it was concluded that up-regulation of miR-142-5p expression could inhibit the growth, invasion, and EMT of RB cells, and promote the apoptosis of RB cells, while down-regulation could reverse. This revealed that miR-142-5p played the role of tumor suppressor gene in RB, which is consistent with its role in many other tumors. Subsequently, in order to further verify the connection between XIST and miR-142-5p, we also carried out rescue experiments. The results showed that Si-XIST could eliminate the promoting effect of proliferation, invasion, EMT of RB cells and the effect of apoptosis by inhibiting the expression of miR-142-5p. The above results suggested that XIST could inhibit the expression of miR-142-5p in RB to affect the proliferation, invasion, apoptosis and EMT of RB cells.

Conclusions

To sum up, as far as we know, this study first provided evidence to reveal that XIST was raised in RB tissues and cell lines, and it was first demonstrated that XIST could play the role of carcinogenic factor in the development of RB tumor by sponging miR-142-5p. These data revealed that XIST might be a potential therapeutic target for RB. Nevertheless, there are still some shortages in this research. We have not carried out *in vivo* nude mice tumorigenesis experiments to reveal the effect of XIST on solid tumor growth. Secondly, the downstream molecular mechanism of miR-142-5p in RB is still unclear, which will be further explored in future studies.

Conflict of Interest

The Authors declare that they have no conflict of interests.

References

- 1) DIMARAS H, KIMANI K, DIMBA EA, GRONSDAHL P, WHITE A, CHAN HS, GALLIE BL. Retinoblastoma. *Lancet* 2012; 379: 1436-1446.
- 2) KIVELA T. Epidemiological challenge for the most common eye cancer: retinoblastoma, a matter of life and death. *Br J eye drops* 2009; 93: 1129-1131.

- 3) DIMARAS H, CORSON, CANADA. Retinoblastoma, a visible tumor of the central nervous system: a review. *J Neurosci Res* 2019; 97: 29-44.
- 4) GUNDITZ K, MÜFTÜOĞLUO, GÜNALP I, ÜNALE, TAÇYILDIZ N. Clinical features, treatment and prognosis of metastatic retinoblastoma. *Ophthalmology* 2006; 113: 1558-1566.
- 5) DONG ZQ, GUO ZY, XIE J. The lncRNA EGFR-AS1 is linked to migration, invasion and apoptosis in glioma cells by targeting miR-133b/RACK1. *Biomed Pharmacother* 2019; 118: 109292.
- 6) XIA H, XIU M, GAO J, JING H. LncRNA PLAC 2 downregulated miR-21 in non-small cell lung cancer and predicted survival. *BMC Pulm Med* 2019; 19: 172.
- 7) LI C, LIU H, YANG J, YANG J, YANG L, WANG Y, YAN Z, SUN Y, SUN X, JIAO B. Long noncoding RNA LINC00511 induced by SP1 accelerates the glioma progression through targeting miR-124-3p/CCND2 axis. *J Cell Mol Med* 2019; 23: 4386-4394.
- 8) PINTACUDA G, YOUNG AN, CERASE A. Functions by structure: focus on long non-coding RNA. *Front Mol Biosci* 2017; 4: 90.
- 9) CUI CL, LI YN, CUI XY, WU X. LncRNA XIST promotes the progression of laryngeal squamous cell carcinoma by sponging miR-144 to regulate IRS1 expression. *Oncol Rep* 2020; 43: 525-535.
- 10) CHENG Z, LUO C, GUO Z. LncRNA-XIST/microRNA-126 sponge mediates cell proliferation and glucose metabolism through the IRS1/PI3K/Akt pathway in glioma. *J Cell Biochem* 2020; 121: 2170-2183.
- 11) HU C, LIU S, HAN M, WANG Y, XU C. Knockdown of lncRNA XIST inhibits retinoblastoma progression by modulating the miR-124/STAT3 axis. *Biomed Pharmacother* 2018; 107: 547-554.
- 12) VENKATESAN N, DEEPA PR, KHETAN V, KRISHNAKUMAR S. Computational and in vitro investigation of miRNA-gene regulations in retinoblastoma pathogenesis: miRNA mimics strategy. *Bioinform Biol Insights* 2015; 9: 89-101.
- 13) DE GRAAF P, GÖRICKÉ S, RODJAN F, GALLUZZI P, MAEDER P, CASTELJINS JA, BRISSE HJ. Guidelines for imaging retinoblastoma: imaging principles and MRI standardization. *Pediatr Radiol* 2012; 42: 2-14.
- 14) ZHENG R, LIN S, GUAN L, YUAN H, LIU K, LIU C, YE W, LIAO Y, JIA J, ZHANG R. Long non-coding RNA XIST inhibited breast cancer cell growth, migration, and invasion via miR-155/CDX1 axis. *Biochem Biophys Res Commun* 2018; 498: 1002-1008.
- 15) SALAMA EA, ADBELTAWAB RE, EL TAYEBI HM. XIST and TSIX: novel cancer immune biomarkers in PD-L1-overexpressing breast cancer patients. *Front Oncol* 2019; 9: 1459.
- 16) CHEN Z, HU X, WU Y, CONG L, HE X, LU J, FENG J, LIU D. Long non-coding RNA XIST promotes the development of esophageal cancer by sponging miR-494 to regulate CDK6 expression. *Biomed Pharmacother* 2019; 109: 2228-2236.
- 17) WANG C, QI S, XIE C, LI C, WANG P, LIU D. Up-regulation of long-term non-coding RNA XIST has anti-cancer effects on epithelial ovarian cancer cells through down-regulation of hsa-miR-214-3p. *J Gynecol Oncol* 2018; 29: e99.
- 18) WANG H, JI X. SMAD6, positively regulated by the DN-M3OS-miR-134-5p axis, confers promoting effects to cell proliferation, migration and EMT process in retinoblastoma. *Cancer Cell Int* 2020; 20: 23.
- 19) NIETO MA, HUANG RY, JACKSON RA, THIERY JP. EMT: 2016. *Cell* 2016; 166: 21-45.
- 20) ROSS JS, FIGGE HL, BUI HX, DEL ROSARIO AD, FISHER HA, NAZEER T, JENNINGS TA, INGLE R, KIM DN. Expression of E-cadherin in prostate cancer biopsies: correlation with tumor grade, DNA content, pathological stage, and clinical outcome. *Mod Pathol* 1994; 7: 835-841.
- 21) BAI H, CHANG Y, LI B, MAO Y, JONAS JB. Effects of lentivirus-mediated astrocyte elevated gene-1 overexpression on proliferation and apoptosis of human retinoblastoma cells. *Acta Ophthalmol* 2019; 97: e397-e402.
- 22) SALMENA L, POLISENO L, TAY Y, KATS L, PANDOLFI PP. CeRNA hypothesis: rosetta stone of hidden RNA language? *Cell* 2011; 146: 353-358.
- 23) YAO R, XU L, WEI B, QIAN Z, WANG J, HUI H, SUN Y. MiR-142-5p regulates pancreatic cancer cell proliferation and apoptosis by regulation of RAP1A. *Pathol Res Pract* 2019; 215: 152416.
- 24) WANG Z, LIU Z, FANG X, YANG H. MiR-142-5p suppresses tumorigenesis by targeting PIK3CA in non-small cell lung cancer. *Cell Physiol Biochem* 2017; 43: 2505-2515.
- 25) JO DH, KIM JH, PARK WY, KIM KW, YU YS, KIM JH. Differential profiles of microRNAs in retinoblastoma cell lines of different proliferation and adherence patterns. *J Pediatr Hematol Oncol* 2011; 33: 529-533.